

Tilt-angle landscapes and temperature dependence of the conductance in biphenyl-dithiol single-molecule junctions

F. Pauly,^{1,*} J. K. Viljas,^{1,2} J. C. Cuevas,^{3,1,2} and Gerd Schön^{1,2}

¹*Institut für Theoretische Festkörperphysik and DFG-Center for Functional Nanostructures, Universität Karlsruhe, D-76128 Karlsruhe, Germany*

²*Forschungszentrum Karlsruhe, Institut für Nanotechnologie, D-76021 Karlsruhe, Germany*

³*Departamento de Física Teórica de la Materia Condensada, Universidad Autónoma de Madrid, E-28049 Madrid, Spain*

(Dated: February 8, 2022)

Using a density-functional-based transport method we study the conduction properties of several biphenyl-derived dithiol (BPDDT) molecules wired to gold electrodes. The BPDDT molecules differ in their side groups, which control the degree of conjugation of the π -electron system. We have analyzed the dependence of the low-bias zero-temperature conductance on the tilt angle φ between the two phenyl ring units, and find that it follows closely a $\cos^2 \varphi$ law, as expected from an effective π -orbital coupling model. We show that the tilting of the phenyl rings results in a decrease of the zero-temperature conductance by roughly two orders of magnitude, when going from a planar conformation to a configuration in which the rings are perpendicular. In addition we demonstrate that the side groups, apart from determining φ , have no influence on the conductance. All this is in agreement with the recent experiment by Venkataraman *et al.* [Nature **442**, 904 (2006)]. Finally, we study the temperature dependence of both the conductance and its fluctuations and find qualitative differences between the examined molecules. In this analysis we consider two contributions to the temperature behavior, one coming from the Fermi functions and the other one from a thermal average over different contact configurations. We illustrate that the fluctuations of the conductance due to temperature-induced changes in the geometric structure of the molecule can be reduced by an appropriate design.

PACS numbers: 73.63.-b, 73.63.Rt

I. INTRODUCTION

In atomic-scale conductors the precise positions of the atoms have a decisive influence on the electronic transport properties.^{1,2,3} In the case of metal-molecule-metal contacts the importance of such details often complicates the reproducibility of the experimental results.^{4,5,6} For this reason statistical analyses of the experimental data, such as conductance histograms, have become indispensable for exploring the charge-transport characteristics of single-molecule contacts.^{5,6,7,8,9,10}

Recently, making use of conductance histograms, Venkataraman *et al.* were able to reveal the influence of molecular conformation on the conductance of single-molecule contacts.¹¹ In their experiments, these authors investigated biphenyl-derived molecules, where different side groups were used to control the tilt angle φ between two phenyl rings. Thereby, the extent of the delocalized π -electron system of the molecules could be varied. They found that the conductance exhibited a characteristic $\cos^2 \varphi$ behavior, as expected from a simple effective π -orbital coupling model.^{12,13}

Motivated by the experiment of Ref. 11, we analyze theoretically the charge-transport properties of three different biphenyl-derived dithiol (BPDDT) molecules connected to gold electrodes. For simplicity, we refer to these molecules as R2, S2, and D2 (Fig. 1). While R2 is the conventional biphenyl, the other two molecules, 2,2'-dimethyl-biphenyl (S2) and 2,6,2',6'-tetramethyl-

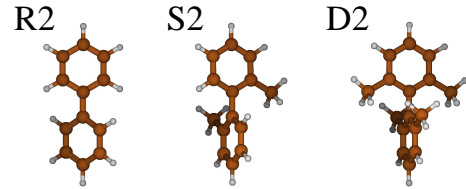


Figure 1: (Color online) Biphenyl molecules R2, S2, and D2. For S2 one hydrogen atom in the ortho position with respect to the ring-connecting carbons in each phenyl ring of R2 is replaced by a methyl group. For D2 also the second ortho-positioned hydrogen is substituted by a methyl group.

biphenyl (D2), differ from R2 by the incorporation of one or two methyl groups in the ortho position with respect to the ring-connecting carbon atoms.

As an important difference to Ref. 11, we bind the molecules R2, S2, and D2 to gold using thiol end groups instead of amino groups. It has recently been shown that amino groups are better suited to establish a reproducible contact of a molecule to a gold electrode.^{5,6} These findings have been explained by the less directional character of the amine-gold bond as compared to the thiol-gold linkage. Nevertheless, thiol groups remain a frequent choice to establish the electrode-molecule contact,^{4,7,10,14} and the molecules R2, S2, and D2 with acetyl-protected sulfur end groups have recently been synthesized.¹⁵ Besides, it is the internal structure of the molecules that is

most important for the charge-transport characteristics discussed below.

In this work we investigate the effect of the degree of π conjugation on the conductance of BPDDT molecules connected to gold electrodes. For this purpose, we describe the electronic structure of the single-molecule contacts at the level of density functional theory (DFT). We demonstrate that, in agreement with the experiments of Ref. 11, a $\cos^2 \varphi$ behavior of the low-bias zero-temperature conductance is obtained. This behavior is by and large independent of the methyl side groups introduced. We find that the breaking of the conjugation reduces the zero-temperature conductance by roughly two orders of magnitude. In addition, we study the temperature dependence of the conductance for all our molecules. For this we take two contributions into account. The first one comes from the broadening of the Fermi functions of the leads, the other one from a thermal average over different geometric configurations. In our analysis we observe that S2 and D2 exhibit a monotonously increasing conductance as a function of temperature, while for R2 the temperature dependence is non-monotonous. Finally, we demonstrate that the temperature-fluctuations of the conductance of single-molecule contacts can be reduced by an appropriate design of the geometric structure of a molecule. This design should aim at stabilizing the molecule with respect to the internal degrees of freedom that are most relevant for its conduction properties. Due to the elimination of uncertainties about the molecule's internal structure in a contact, a more reliable comparison of experimental and theoretical results on the charge-transport characteristics of single-molecule junctions can be expected.

The rest of the paper is organized as follows. In Sec. II we outline the methods used to compute the electronic structure, geometry, and conductance of the molecular contacts discussed below. Sec. III is devoted to the discussion of the results for the conductance of the three BPDDT molecules, in particular their tilt-angle dependence and temperature behavior. Technical details on these issues are deferred to Apps. A and B. Finally, we summarize our results in the conclusions, Sec. IV.

II. THEORETICAL MODEL

In this section we present the methods applied in our work. These include the procedures for computing the electronic structure, the contact geometries, and the conduction properties of the molecular contacts. For further details on our method we refer the reader to Refs. 16,17,18.

A. Electronic structure and contact geometries

For the determination of the electronic structure we employ DFT as implemented in the RI-DFT module

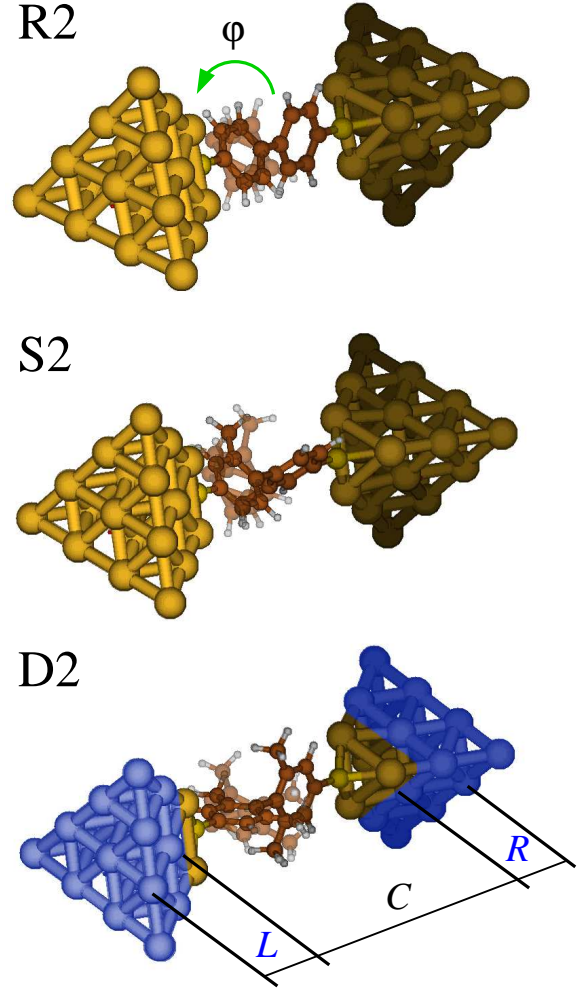


Figure 2: (Color online) Molecules R2, S2, and D2 contacted at both ends to Au [111] electrodes via a sulfur atom in a three-fold binding position. Faintly overlaid on the ground-state structure of the single-molecule contacts are geometries, where the left ring is rotated to $\varphi = \varphi_0 \pm 30^\circ$. Here φ , as indicated for R2, is the tilt angle between the planes of the two phenyl rings, and φ_0 is its ground-state value. The division of the junctions into the left (*L*), central (*C*), and right (*R*) regions, of relevance in the conductance calculations, is also shown.

of the quantum chemistry package TURBOMOLE v5.7 (Refs. 19,20). All our calculations, including the electrode description, are done within TURBOMOLE's standard Gaussian basis set, which is of split-valence quality with polarization functions on all non-hydrogen atoms.^{20,21,22} As the exchange-correlation functional we use BP86 (Refs. 23,24,25). All calculations were performed in a closed-shell formalism, and total energies were converged to a precision of better than 10^{-6} atomic units.

Our contact geometries are displayed in Fig. 2. For their determination we calculate at first the geometric

structure of a gold (Au) [111] pyramid with a thiolated benzene molecule on top. This pyramid consists of three layers of Au with 3, 6, and 10 atoms. The tip atom of the pyramid is missing so that the sulfur (S) atom of the benzene binds to a threefold hollow site on top of the Au structure. We relax all atomic positions except for the layers containing 6 and 10 atoms, which are kept fixed. In particular, their lattice constant is set to 4.08 Å, the experimental bulk atomic distance of gold. Next, we compute the geometry of the biphenyl molecules R2, S2, and D2 of Fig. 1 with the hydrogen atoms in the position 4 and 4' substituted by sulfur atoms, which are bonded to a single gold atom, respectively. For each of these molecules we replace the single Au atoms on each side with the previously mentioned Au [111] pyramids, where the thiolated benzene molecule has been removed. In this process we take care that the sulfur atoms of the biphenyl molecules are in the old positions of the sulfur atoms of the thiolated benzene on top of the Au pyramids, and that the S–S molecular axis and the [111] direction are aligned. The ground-state contact geometry is subsequently obtained by relaxing the complete structure, where we keep only the terminal two gold layers on each side fixed (atoms shown in blue in Fig. 2). As above, the lattice constant in these layers is 4.08 Å. The relaxations thus include all atoms of the molecule, two sulfur atoms, and six Au atoms, three on each side. In the determination of the contact geometries we let the maximum norm of the Cartesian gradient decay to values below 10^{-4} atomic units.

B. Transmission function

To compute the charge transport we apply a method based on standard Green's function techniques and the Landauer formula expressed in a local nonorthogonal basis.^{17,26,27} The local basis allows us to partition the basis states into left (L), central (C), and right (R) parts, according to a division of the contact geometry. Thus the Hamiltonian (or single-particle Fock) matrix \mathbf{H} , and analogously the overlap matrix \mathbf{S} , can be written in the block form

$$\mathbf{H} = \begin{pmatrix} \mathbf{H}_{LL} & \mathbf{H}_{LC} & \mathbf{0} \\ \mathbf{H}_{CL} & \mathbf{H}_{CC} & \mathbf{H}_{CR} \\ \mathbf{0} & \mathbf{H}_{RC} & \mathbf{H}_{RR} \end{pmatrix}.$$

Within the Green's function method the energy-dependent transmission $\tau(E)$ is expressed as²⁸

$$\tau(E) = \text{Tr}[\mathbf{\Gamma}_L \mathbf{G}_{CC}^r \mathbf{\Gamma}_R \mathbf{G}_{CC}^a], \quad (1)$$

with the Green's functions

$$\mathbf{G}_{CC}^r(E) = [\mathbf{E} \mathbf{S}_{CC} - \mathbf{H}_{CC} - \mathbf{\Sigma}_L^r(E) - \mathbf{\Sigma}_R^r(E)]^{-1}$$

and $\mathbf{G}_{CC}^a = [\mathbf{G}_{CC}^r]^\dagger$, the self energies

$$\mathbf{\Sigma}_X^r(E) = (\mathbf{H}_{CX} - \mathbf{E} \mathbf{S}_{CX}) \mathbf{g}_{XX}^r(E) (\mathbf{H}_{XC} - \mathbf{E} \mathbf{S}_{XC}), \quad (2)$$

the scattering rate matrices $\mathbf{\Gamma}_X(E) = -2\text{Im}[\mathbf{\Sigma}_X^r(E)]$, and the electrode Green's function \mathbf{g}_{XX}^r , where $X = L, R$.

In Fig. 2 we show how we divide our contacts into the L , C , and R regions. In this way we obtain \mathbf{H}_{CC} and \mathbf{S}_{CC} for the C region, which consists of the BPDDT molecule and three gold atoms on each side of the junction. The L and R regions are made up of the two terminal gold layers on each side of the gold pyramids (blue shaded atoms of Fig. 2), which have been kept fixed to bulk atomic distances in the geometry relaxations. The matrices \mathbf{H}_{CX} and \mathbf{S}_{CX} , extracted from these finite contact geometries, serve as the couplings to the electrodes in the construction of $\mathbf{\Sigma}_X^r(E)$. However, the electrode Green's functions $\mathbf{g}_{XX}^r(E)$ in Eq. (2) are modeled as surface Green's functions of ideal semi-infinite electrodes. In order to obtain these surface Green's functions, we compute the electronic structure of a spherical gold cluster with 429 atoms. From this we extract the Hamiltonian and overlap matrix elements connecting the atom in the origin of the cluster to all its neighbors and, using these "bulk parameters", construct a semi-infinite crystal which is infinitely extended perpendicular to the transport direction. The surface Green's functions are then calculated from this crystal using the so-called decimation technique.²⁹ We have checked that the electrode construction in the employed nonorthogonal basis set has converged with respect to the size of the Au cluster, from which we extract our parameters.¹⁶ In this way we describe the whole system consistently within DFT, using the same nonorthogonal basis set and exchange-correlation functional everywhere.

We assume the Fermi energy E_F to be fixed by the gold leads. From the Au₄₂₉ cluster we obtain a Fermi energy for gold of $E_F = -5.0$ eV, which is chosen to lie halfway between the levels of the highest occupied molecular orbital (HOMO) and the lowest unoccupied molecular orbital (LUMO) of the cluster of -4.96 and -5.01 eV, respectively.

C. Conductance

The low-bias conductance in the Landauer formalism is given by^{28,30}

$$G_\varphi(T) = G_0 \int_{-\infty}^{\infty} dE \left[-\frac{\partial}{\partial E} f(E) \right] \tau_\varphi(E). \quad (3)$$

In this expression T is the temperature, $G_0 = 2e^2/h$ is the conductance quantum, $\tau_\varphi(E)$ is the energy-dependent transmission [Eq. (1)], and $f(E) = 1/[e^{-(E-E_F)/k_B T} + 1]$ is the Fermi function with Boltzmann's constant k_B . The factor $-\partial f(E)/\partial E$ is the so-called thermal broadening function.²⁸ For zero temperature, Eq. (3) reduces to $G_\varphi(T = 0\text{ K}) = G_0 \tau_\varphi(E_F)$. Here and henceforth we index G and τ with φ , which parameterizes different geometrical contact configurations. In our case these configurations correspond to different

molecular conformations with the tilt angle φ between two phenyl rings (Fig. 2). At finite temperature, tilt angles φ differing from the minimum-energy, ground-state value can be accessed. We account for this additional temperature-dependent contribution to the conductance by the thermal average^{30,31}

$$\bar{G}(T) = \langle G_\varphi(T) \rangle_\varphi \quad (4)$$

with $\langle \dots \rangle_\varphi = \int d\varphi e^{-E_\varphi/k_B T} (\dots) / \int d\varphi e^{-E_\varphi/k_B T}$. In this expression E_φ is the energy of the metal-molecule-metal contact for angle φ . The contribution of $G_\varphi(T)$ to $\bar{G}(T)$ can be seen as a “electronic” or “lead-induced” temperature dependence, because it follows from the Fermi functions of the electrodes. Its determination is discussed in App. A. On the other hand, the φ average represents a “configuration-induced” contribution to $\bar{G}(T)$. For the later discussion, we also introduce the variance

$$\delta G(T) = \sqrt{\langle (G_\varphi(T) - \bar{G}(T))^2 \rangle_\varphi} \quad (5)$$

that describes the fluctuations of the conductance.

III. RESULTS AND DISCUSSION

Let us first discuss some properties of the isolated molecules (Fig. 1). For R2, S2, and D2 we obtain phenyl-ring tilt angles φ of 36.4° , 90.0° , and 90.0° , respectively. The tilt angle of R2 is a result of the interplay between the π conjugation, which tries to flatten the structure ($\varphi = 0^\circ$), and the steric repulsion of the hydrogen atoms in the ortho positions with respect to the ring-connecting carbons, which favors tilt angles close to $\varphi = 90^\circ$ (Ref. 32). The methyl groups introduced in S2 and D2 increase the steric repulsion and cause a larger φ . As a consequence, the conjugation between the phenyl rings is largely broken in S2 and D2, whereas R2 still preserves a reasonable degree of delocalization of the π -electron system over the whole molecule. This fact is clearly reflected in the change of the HOMO-LUMO gaps Δ , which are 3.85 eV for R2, 4.74 eV for S2, and 4.70 eV for D2. Thus, Δ increases by roughly 1 eV when going from R2 to S2 or D2. This suggests that the molecules S2 and D2 will show a more insulating behavior than R2, when they are incorporated into a molecular contact.

Now, we study the geometric structure of the metal-molecule-metal contacts. In Fig. 2 we show the biphenyl molecules contacted at both ends to gold electrodes via sulfur bonds, where the sulfur resides on the threefold hollow position of Au [111] pyramids. The molecular conformation in the junction is very similar to the ground-state structure of the isolated molecule, as there is no internal stress on the molecule in this binding position.^{16,33} In particular, we obtain ground-state tilt angles φ_0 of 33.8° , 89.3° , and 89.7° for R2, S2, and D2, respectively.

In order to analyze the conduction properties of these molecular junctions, we have computed the transmission

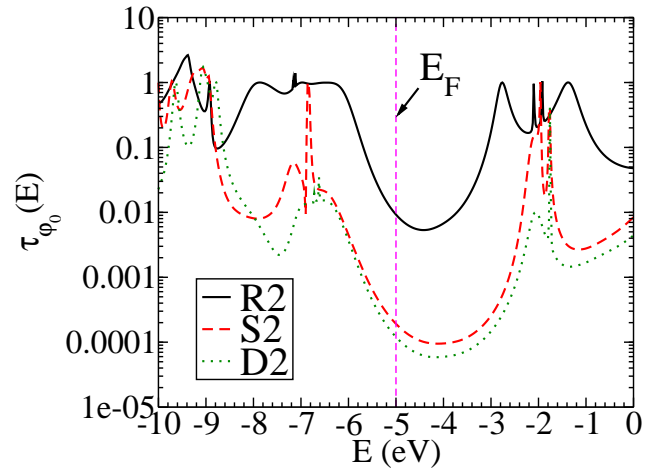


Figure 3: (Color online) Transmission $\tau_{\varphi_0}(E)$ as a function of energy E for the ground-state geometries of the contacts shown in Fig. 2. The zero-temperature conductances $G_{\varphi_0}(T = 0 \text{ K})$ of molecules R2, S2, and D2 are $9.2 \times 10^{-3} G_0$, $1.9 \times 10^{-4} G_0$, and $1.2 \times 10^{-4} G_0$, respectively. The vertical dashed line indicates the Fermi energy E_F .

$\tau_{\varphi_0}(E)$ as a function of energy for the ground-state geometries of the contacts (angle φ_0 in Fig. 2). The results are plotted in Fig. 3, and our transmission curve for R2 agrees well with previous theoretical studies.³⁴ Obviously, $\tau_{\varphi_0}(E)$ is dominated by a gap around the Fermi energy E_F , which reflects the HOMO-LUMO gaps Δ of the isolated molecules. As can be expected due to the similar geometric conformations of molecules S2 and D2 with $\varphi_0 \approx 90^\circ$, their transmission curves closely resemble each other. However, the most important observation to be made from Fig. 3 is the great reduction of the transmission $\tau_{\varphi_0}(E_F)$ at the Fermi energy for S2 and D2 as compared to R2. In particular, the conductance of S2 (D2) is lower than that of R2 by a factor of 48 (77), i.e. roughly by two orders of magnitude. This clearly reveals the importance of the conjugated π -electron system for the charge transport in biphenyl molecules.¹³ In addition, it shows that the conductance can be tailored by means of adequate side groups that force the biphenyl molecules to adopt different molecular conformations.¹¹

To investigate the dependence of the conductance on the tilt angle in more detail, we have continuously varied φ for all the contacts. We do this by rotating one of the phenyl rings with respect to the other, as illustrated in Fig. 2, without relaxing the contact geometries for tilt angles deviating from φ_0 . By changing φ , we obtain the results depicted in Fig. 4, where the total energy E_φ and the conductance $G_\varphi(T = 0 \text{ K})$ are plotted as a function of φ (Ref. 35,36,37). We explore the tilt-angle intervals of $[0^\circ, 360^\circ[$ for R2, $[60^\circ, 300^\circ]$ for S2, and $[60^\circ, 120^\circ]$ for D2 (Ref. 38). In each case the angular resolution is $\Delta\varphi = 2^\circ$.

In the energy curve E_φ of molecule R2 there are eight extrema visible, four minima and four maxima. They

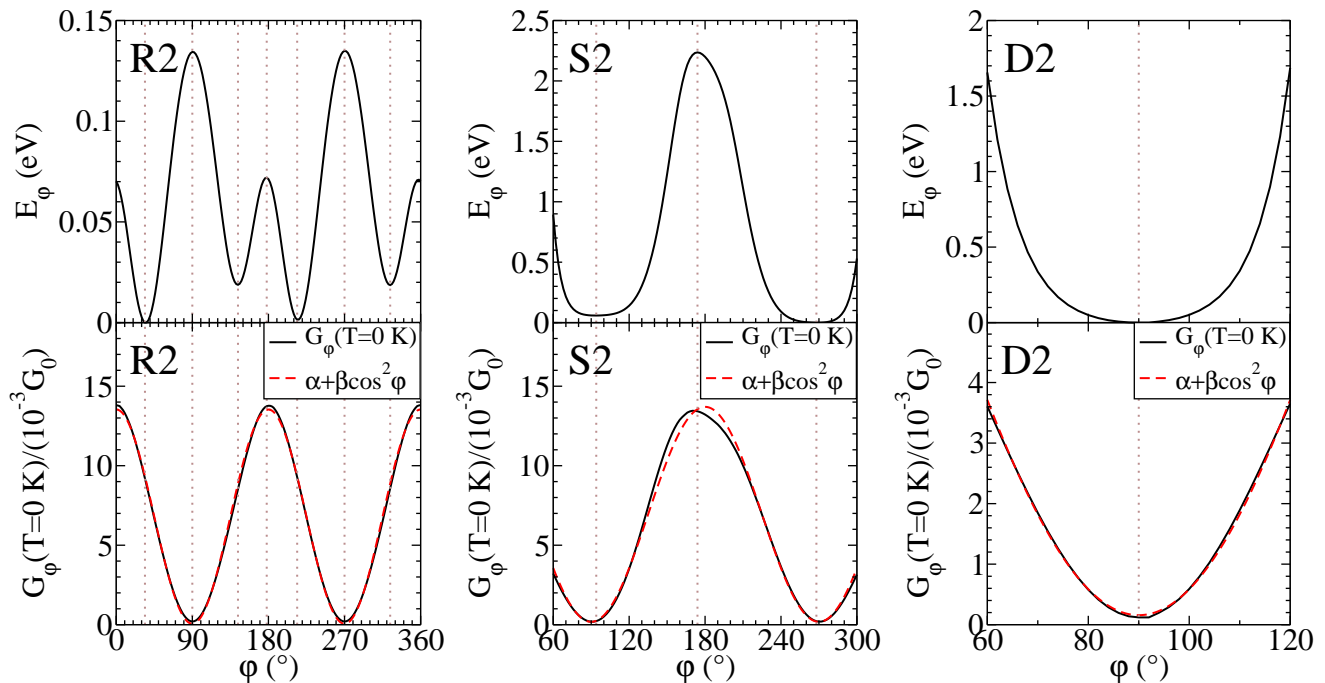


Figure 4: (Color online) Landscapes of the total energy E_φ (upper panels) and the conductance $G_\varphi(T = 0 \text{ K})$ (lower panels) as a function of tilt angle φ for the molecules R2, S2, and D2. Dotted vertical lines indicate positions of extrema in E_φ for the respective molecules (all panels). In the lower panels a function of the form $\alpha + \beta \cos^2 \varphi$ has been fitted to $G_\varphi(T = 0 \text{ K})$ (see the legend). For the fit parameters we obtain $\alpha = 5.95 \times 10^{-5} G_0$ and $\beta = 1.35 \times 10^{-2} G_0$ (R2), $\alpha = 1.81 \times 10^{-4} G_0$ and $\beta = 1.35 \times 10^{-2} G_0$ (S2), and $\alpha = 1.58 \times 10^{-4} G_0$ and $\beta = 1.42 \times 10^{-2} G_0$ (D2).

are located at 34° , 144° , 214° , and 324° for the energy minima and 90° , 178° , 270° , and 358° for the maxima. Due to the symmetry of the biphenyl molecule, one would expect a 180° periodicity and a mirror symmetry of both E_φ and $G_\varphi(T = 0 \text{ K})$ with respect to 0° (or equivalently 90° , 180° , or 270°). While the 180° periodicity is present for E_φ , the mirror symmetry is violated, as one can see in Fig. 4. The reason for this is that the hydrogen atoms have been fixed in their positions with respect to the phenyl rings as obtained for the ground-state tilt angle φ_0 . They are standing slightly away from the phenyl ring planes in this position, which leads to the observed violation of the mirror symmetry.^{37,39} Contrary to E_φ , all expected symmetries are restored for the conductance. In particular, $G_\varphi(T = 0 \text{ K})$ possesses only two minima at 90° and 270° and two maxima at 0° and 180° . As a function of tilt angle, the conductance changes from $2.0 \times 10^{-4} G_0$ in the minima to $1.4 \times 10^{-2} G_0$ in the maxima, that is, it changes by a factor of 70.

In the case of molecules S2 and D2, $G_\varphi(T = 0 \text{ K})$ follows closely the shape of the energy curve. For S2 there are two minima in E_φ at 94° and 268° with conductances of $2.2 \times 10^{-4} G_0$, separated by a local maximum at 174° with a conductance of $1.3 \times 10^{-2} G_0$. This corresponds to a ratio of 60 between the maximum and minimum conductance. D2 exhibits an energy minimum at 90° and the conductance at this point is $1.2 \times 10^{-4} G_0$.

The close agreement of the minimal conductances for R2, S2, and D2 (Figs. 3 and 4) is remarkable. In the conductance minima the conformations of these molecules are the same, except for their different side groups and their slightly varying orientations with respect to the gold electrodes. These observations demonstrate that the side groups control the conformation, but otherwise have little impact on the zero-temperature conductance. This is in agreement with the experimental observations of Ref. 11.

The large ratios between maximal and minimal conductances (70 for R2 and 60 for S2) reported above highlight the relevance of the extent of the conjugated π -electron system on the conduction properties of the biphenyl molecules. In order to further investigate this, we have fitted the $G_\varphi(T = 0 \text{ K})$ curves of Fig. 4 to functions of the form $\alpha + \beta \cos^2 \varphi$ (see the figure caption for the obtained fit parameters). A behavior $G_\varphi(T = 0 \text{ K})/G_0 \propto \cos^2 \varphi$ is expected if the coupling between the π -electron systems of the two phenyl rings plays the dominant role in charge transport, as discussed in more detail in App. B. For all three molecules our fit matches $G_\varphi(T = 0 \text{ K})$ very well. What is more, we obtain a very similar parameter β for all of them. On the other hand, the small but positive values of α indicate that the conductance at perpendicular tilt angles ($\varphi = 90^\circ$ or 270°) does not vanish entirely, as a pure $\cos^2 \varphi$ dependence would suggest. This observation was also made in

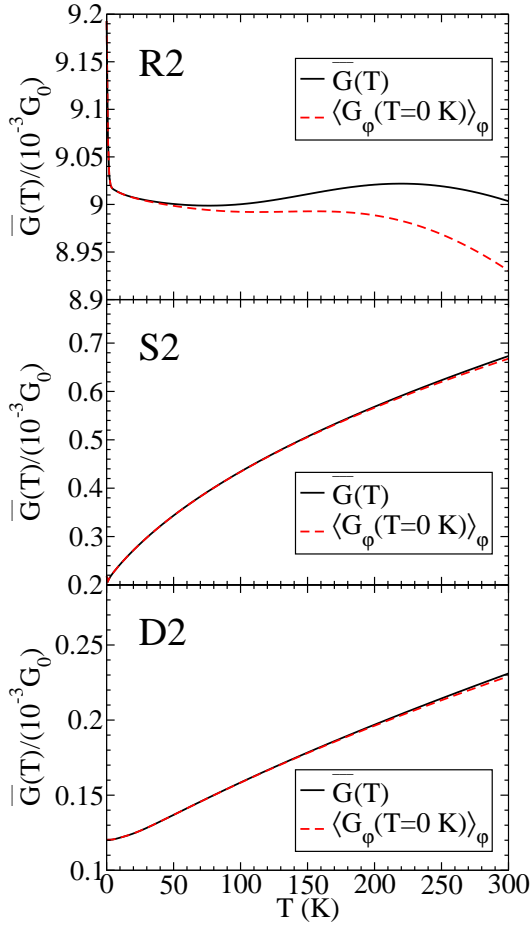


Figure 5: (Color online) Behavior of the conductances $\bar{G}(T)$ and $\langle G_\varphi(T=0\text{ K}) \rangle_\varphi$ as a function of temperature T for the molecules R2, S2, and D2.

Ref. 11. The absence of a complete blockade of the transport can be understood by the presence of other than the π - π couplings.

Next, we analyze the behavior of the conductance with respect to temperature. In addition to $\bar{G}(T) = \langle G_\varphi(T) \rangle_\varphi$ [Eq. (4)] we study $\langle G_\varphi(T=0\text{ K}) \rangle_\varphi$. In this way we can quantify the lead-induced contribution to the temperature dependence of $\bar{G}(T)$. To perform the average $\langle G_\varphi(T=0\text{ K}) \rangle_\varphi$ we use the energy and conductance landscapes E_φ and $G_\varphi(T=0\text{ K})$ of the gold-molecule-gold contacts as shown in Fig. 4. For $\bar{G}(T)$, instead, we have calculated the transmission function for each angle in an interval around E_F in order to obtain $G_\varphi(T)$ (see the explanations in Sec. II and App. A).^{40,41}

The temperature-dependent conductances $\bar{G}(T)$ and $\langle G_\varphi(T=0\text{ K}) \rangle_\varphi$ are plotted in Fig. 5 for the molecules R2, S2, and D2 for temperatures T between 0 and 300 K. With respect to the behavior of $\bar{G}(T)$ we observe qualitative differences for the three molecules considered. S2 and D2 exhibit a monotonously increasing conductance $\bar{G}(T)$ with increasing T . In contrast, after an initial drop, a

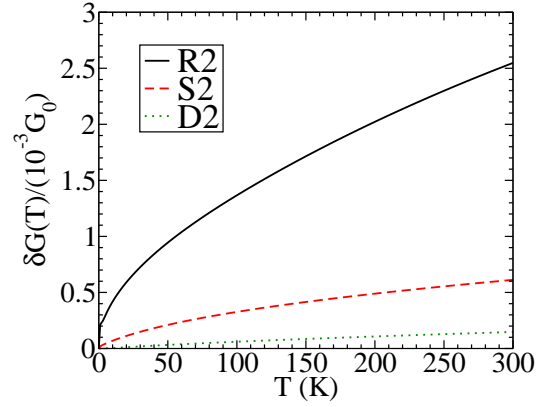


Figure 6: (Color online) Fluctuations $\delta G(T)$ of the conductance as a function of temperature T for the molecules R2, S2, and D2.

non-monotonous weak temperature dependence is found for R2.

The small differences between $\bar{G}(T)$ and $\langle G_\varphi(T=0\text{ K}) \rangle_\varphi$ for S2 and D2 indicate that for these molecules the lead-induced contribution to the temperature dependence can be neglected as compared to the configurational one. The monotonous increase of $\bar{G}(T)$ can therefore be understood by E_φ and $G_\varphi(T=0\text{ K})$ (Fig. 4). The ground-state or equivalently zero-temperature configurations for both molecules correspond to conformations with minimal conductances. Therefore elevated temperatures give access to conformations with higher conductance values, resulting in the observed steady increase of $\bar{G}(T)$. For molecule R2 the situation is different. Here, the energy E_{φ_0} at the ground-state tilt angle of $\varphi_0 = 34^\circ$ does not correspond to a minimum of $G_\varphi(T=0\text{ K})$. Elevated temperatures give access to both higher and lower conductances and, as a result, $\langle G_\varphi(T=0\text{ K}) \rangle_\varphi$ exhibits no clear trend. The differences between $\bar{G}(T)$ and $\langle G_\varphi(T=0\text{ K}) \rangle_\varphi$ signify that for R2 both contributions to the temperature dependence of the conductance, namely the lead-induced and the configuration-induced ones, play an equally important role.⁴²

Finally we analyze the fluctuations of the conductance $\delta G(T)$ [Eq. (5)], which we have plotted in Fig. 6 for temperatures T ranging between 0 and 300 K. In each case $\delta G(T)$ increases monotonously with T . This is clear, as finite temperatures give access to conductances differing from the ground-state conductance $G_{\varphi_0}(T=0\text{ K})$ (Fig. 4). It is also evident from Fig. 6 that $\delta G(T)$ is largest for R2 and smallest for D2. Indeed, because of its two methyl side groups, D2 is the most rigid of the three molecules with respect to ring tilts, while R2 can access a large range of conductance values due to its shallow energy landscape (Fig. 5). Since S2 has only one methyl side group, it is an intermediate case. From Fig. 6 we obtain the temperature-fluctuation ratios

$\delta G_{R2}(T)/\delta G_{S2}(T) = 4.2$ and $\delta G_{S2}(T)/\delta G_{D2}(T) = 4.2$ for $T = 300$ K, where $\delta G_{X2}(T)$ refers to the variance of the molecule X2.

In experiments with molecular junctions the conductance in the last plateau of an opening curve is generally attributed to that of a single molecule. In practice the measured conductances are always time averages over any fast fluctuations of the contact geometry, in particular the internal conformations of the molecule. In terms of our definitions, $\bar{G}(T)$ represents such a time average for a given contact realization, while $\delta G(T)$ describes the fast fluctuations.

The time-averaged single-molecule conductance may vary considerably from one junction realization to another.^{4,6,9} These variations, and hence the peak widths in conductance histograms, can be attributed to two types of factors. The first one is due to changes at the molecule-electrode interface and in the contact environment, and the second one is due to modifications of the molecule's internal geometric structure. Concerning the first contribution, the surfaces of the metallic electrodes are atomically rough and disordered, and the molecule binds differently to the electrodes in every realization of the junction.^{6,10,43} As a result, the interface-related variability of the single-molecule conductance is hard to control at present, although more reproducible results can be achieved by a proper choice of the binding groups.⁵ Regarding the second point, however, the recent possibilities of chemical synthesis allow the structure of a molecule to be designed. In order to measure the conductance of a single molecule more reproducibly, such a design should aim at making the molecule "rigid" (for example by means of side groups, as in the examples considered above).^{11,16,33} In this way the variability due to the changes in the internal structure is reduced, because the bonded molecules stay closer to their ground-state conformations in isolation.

In our analysis several simplifying assumptions have been made. In particular, we have concentrated on a certain realization of a single-molecule junction (Fig. 2) and all temperature-induced changes at the electrode-molecule interface have been neglected. Furthermore, only one configurational degree of freedom of the molecule, the tilt angle φ , has been taken into account, and we treated it as a classical variable. Nevertheless, our analysis serves to illustrate the importance of the temperature-related effects on the average conductance and its fluctuations, and how these can be controlled by an appropriate design of the molecules. By reducing uncertainties about the contact geometries in this way, comparisons between theoretical and experimental results can be made with a higher degree of confidence.

IV. CONCLUSIONS

In conclusion, we studied the charge-transport properties of different dithiolated biphenyl derivatives. We

showed by means of density-functional-based methods that the conduction properties of these molecules are dominated by the degree of π -electron delocalization. A broken conjugation, induced by side groups, was found to suppress the conductance by roughly two orders of magnitude. By varying the tilt angle φ between the different phenyl rings, we observed a clear $\cos^2 \varphi$ behavior of the zero-temperature conductance. However, the suppression of the conductance for perpendicular ring configurations is not complete due to the presence of other than π - π couplings between the phenyl rings. We showed that the methyl side groups in the biphenyl molecules control the conformation, but they have little impact on the zero-temperature conductance otherwise. All these findings are in agreement with the experimental results of Ref. 11.

Based on the energy landscapes with respect to ring tilts, we also determined the temperature dependence of the conductance. Here we considered two different contributions. The first one originates from the Fermi functions of the leads, while the other one is due to a thermal average over different contact configurations. We observed qualitatively different temperature characteristics for the well-conjugated biphenyl molecule as compared to the molecules whose conjugation was broken by means of methyl side groups. Furthermore, we illustrated that an appropriate design can help to reduce temperature-induced conductance fluctuations by stabilizing a molecule in a conformation close to its ground-state structure in isolation. In this way uncertainties with respect to the molecule's internal structure are reduced, and a more reliable comparison between theoretically and experimentally determined charge-transport properties of single-molecule junctions seems possible.

Acknowledgments

We acknowledge stimulating discussions with Marcel Mayor and members of the group for Theoretical Quantum Chemistry at the Universität Karlsruhe, in particular Uwe Huniar and Dmitriy Rappoport. In addition we thank Reinhart Ahlrichs for providing us with TURBOMOLE. This work was financially supported by the Helmholtz Gemeinschaft (Contract No. VH-NG-029), by the DFG within the CFN, and by the EU network BI-MORE (Grant No. MRTN-CT-2006-035859). We thank the INT at the FZK for the provision of computational facilities.

Appendix A: TEMPERATURE DEPENDENCE OF THE CONDUCTANCE

In order to evaluate the temperature behavior of the conductance $G_\varphi(T)$ as defined in Eq. (3), we make a Sommerfeld expansion.⁴⁴ For this we compute $\tau_\varphi(E)$ [Eq. (1)] at 11 equally spaced points in the energy in-

interval $-0.5\text{ eV} \leq E - E_F \leq 0.5\text{ eV}$ around the Fermi energy E_F for every tilt angle φ . This interval is chosen large enough that the thermal broadening function²⁸

$$b(E, T) = -\frac{\partial}{\partial E} f(E) = \frac{1}{4k_B T} \text{sech}^2 \left(\frac{E - E_F}{2k_B T} \right)$$

has decayed to small values even for the highest temperatures considered. (For example one gets $b(E_F \pm 0.5\text{ eV}, 300\text{ K})/b(E_F, 300\text{ K}) = 1.59 \times 10^{-8}$.) Next, we fit a polynomial of order $N = 10$ to $\tau_\varphi(E)$ at these energy points according to

$$\tau_\varphi(E) = \sum_{n=0}^N \tau_\varphi^{(n)} (E - E_F)^n.$$

With the coefficients $\tau_\varphi^{(n)} = d^n \tau_\varphi(E)/dE^n|_{E=E_F}/n!$ determined from the least squares fit [where in particular $\tau_\varphi^{(0)} = \tau_\varphi(E_F)$], the temperature dependence of $G_\varphi(T)$ is given as

$$G_\varphi(T) = G_0 \left[\tau_\varphi^{(0)}(\varphi) + \sum_{m=1}^{\lfloor N/2 \rfloor} \left(2 - 2^{2(1-m)} \right) \times \zeta(2m) (2m)! \tau_\varphi^{(2m)} (k_B T)^{2m} \right]. \quad (\text{A1})$$

In this expression $\lfloor N/2 \rfloor$ is the largest integer smaller than or equal to $N/2$ and $\zeta(x)$ is the Riemann zeta function.

Appendix B: EFFECTIVE π -ORBITAL COUPLING MODEL

The dependence of charge transfer on the tilt angle φ between two phenyl rings has been inspected previously in Refs. 12,13. In this appendix we discuss explicitly, how the $\cos^2 \varphi$ behavior of the conductance can be understood based on an effective π -orbital coupling model within the Green's function formalism.

For this purpose we bring the transmission function $\tau_\varphi(E)$ [Eq. (1)] into a slightly different form, following Ref. 17. We assume that the C part of our contacts can be divided into two regions 1 and 2, where region 1 (2) is not coupled to the R (L) part of the system via direct

hoppings or overlaps. Furthermore, regions 1 and 2 are connected to each other by $\mathbf{t}_{12} = \mathbf{H}_{12} - E\mathbf{S}_{12}$. Then we may write

$$\tau_\varphi(E) = \text{Tr} [\mathbf{A}_{11} \mathbf{T}_{12} \mathbf{A}_{22} \mathbf{T}_{21}], \quad (\text{B1})$$

where $\mathbf{A}_{11} = i(\mathbf{g}_{11}^r - \mathbf{g}_{11}^a)$ and $\mathbf{g}_{11}^r = [\mathbf{g}_{11}^a]^\dagger = [\mathbf{E}\mathbf{S}_{11} - \mathbf{H}_{11} - (\boldsymbol{\Sigma}_L^r)_{11}]^{-1}$ are the spectral density and the Green's functions of region 1 in the absence of \mathbf{t}_{12} , $\mathbf{T}_{12} = \mathbf{t}_{12} + \mathbf{t}_{12} \mathbf{G}_{21}^r \mathbf{t}_{12}$, and $\mathbf{G}_{21}^r = (\mathbf{G}_{CC}^r)_{21}$. Similar expressions hold for \mathbf{A}_{22} and \mathbf{T}_{21} .

In our case, the regions 1 (2) are made up of all atoms in the first (second) phenyl ring plus the sulfur and three gold atoms to the left (right) in region C (Fig. 2). To simplify the discussion, we consider the electronic structure of the molecule in the junctions as separable into σ and π valence electrons, a procedure called π -electron approximation.⁴⁵ Furthermore, we concentrate on the couplings between those $2p$ orbitals on the ring-connecting carbon atoms, which contribute to the π -electron system. These are oriented perpendicular to the respective phenyl rings, and are thus rotated by the angle φ with respect to each other. The indices 1 and 2 then refer to these $2p$ orbitals, and the matrices in Eq. (B1) become scalars. Within an extended Hückel model H_{12} is proportional to the overlap S_{12} (Refs. 46,47,48) and the scalar coupling element $t_{12}(\varphi) = H_{12}(\varphi) - ES_{12}(\varphi)$ at tilt angle φ is seen to be proportional to $\cos \varphi$.

Because the Fermi energy of gold is located in the HOMO-LUMO gap of the organic molecules (Fig. 3), \mathbf{G}_{21}^r can be assumed to be small at E_F . Therefore $T_{12}(\varphi) \approx t_{12}(\varphi)$. Since the φ dependence of A_{11} (A_{22}) can be expected to be small, the $\cos^2 \varphi$ behavior of the zero-temperature conductance follows from Eqs. (3) and (B1)

$$G_\varphi(T = 0\text{ K}) = G_0 \tau_\varphi(E_F) \approx |t_{12}(\varphi)|^2 A_{11} A_{22}.$$

Here all energy-dependent quantities are evaluated at E_F .

Small deviations from the $\cos^2 \varphi$ dependence of $G_\varphi(T = 0\text{ K})$ can be expected due to higher-order terms in the expansion of T_{12} or other than the π - π couplings in \mathbf{t}_{12} . These include for example σ - σ couplings of the ring-connecting carbon atoms and next-nearest-neighbor couplings between regions 1 and 2.

* Electronic address: Fabian.Pauly@kit.edu

¹ N. Agraït, A. Levy Yeyati, and J. M. van Ruitenbeek, Phys. Rep. **377**, 81 (2003).

² Y. Hu, Y. Zhu, H. Gao, and H. Guo, Phys. Rev. Lett. **95**, 156803 (2005).

³ F. Pauly, M. Dreher, J. K. Viljas, M. Häfner, J. C. Cuevas, and P. Nielaba, Phys. Rev. B **74**, 235106 (2006).

⁴ J. Reichert, R. Ochs, D. Beckmann, H. B. Weber,

M. Mayor, and H. v. Löhneysen Phys. Rev. Lett. **88**, 176804 (2002).

⁵ L. Venkataraman, J. E. Klare, I. W. Tam, C. Nuckolls, M. H. Hybertsen, and M. L. Steigerwald, Nano Lett. **6**, 458 (2006).

⁶ J. Ulrich, D. Esrail, W. Pontius, L. Venkataraman, D. Miliar, and L. H. Doerrer, J. Phys. Chem. B, **110**, 2462 (2006).

⁷ X. D. Cui, A. Primak, X. Zarate, J. Tomfohr, O. F. Sankey,

- A. L. Moore, T. A. Moore, D. Gust, G. Harris, and S. M. Lindsay, *Science* **294**, 571 (2001).
- ⁸ R. H. M. Smit, Y. Noat, C. Untiedt, N. D. Lang, M. C. van Hemert, J. M. van Ruitenbeek, *Nature* **419**, 906 (2002).
 - ⁹ B. Xu and N. J. Tao, *Science* **301**, 1221 (2003).
 - ¹⁰ Z. Li, I. Pobelov, B. Han, T. Wandlowski, A. Błaszczuk, and M. Mayor, *Nanotechnology* **18**, 044018 (2007).
 - ¹¹ L. Venkataraman, J. E. Klare, C. Nuckolls, M. H. Hybertsen, and M. L. Steigerwald, *Nature* **442**, 904 (2006).
 - ¹² S. Woitellier, J. P. Launay, and C. Joachim, *Chem. Phys.* **131**, 481 (1989).
 - ¹³ M. P. Samanta, W. Tian, S. Datta, J. I. Henderson, and C. P. Kubiak, *Phys. Rev. B* **53**, R7626 (1996).
 - ¹⁴ E. Lörtscher, J. W. Ciszek, J. Tour, and H. Riel, *Small* **2**, 973 (2006).
 - ¹⁵ A. Shaporenko, M. Elbing, A. Błaszczuk, C. von Hänisch, M. Mayor, and M. Zharnikov, *J. Chem. Phys.* **110**, 4307 (2006).
 - ¹⁶ F. Pauly, PhD thesis, Institut für Theoretische Festkörperphysik, Universität Karlsruhe, Karlsruhe (2007); F. Pauly *et al.*, to be published (2007).
 - ¹⁷ S. Wohlthat, F. Pauly, J. K. Viljas, J. C. Cuevas, and G. Schön, arXiv:cond-mat/0702477.
 - ¹⁸ J. K. Viljas, F. Pauly, and J. C. Cuevas, arXiv:0704.0408.
 - ¹⁹ R. Ahlrichs, M. Bär, M. Häser, H. Horn, and C. Kölmel, *Chem. Phys. Lett.* **162**, 165 (1989).
 - ²⁰ K. Eichkorn, O. Treutler, H. Öhm, M. Häser, and R. Ahlrichs, *Chem. Phys. Lett.* **242**, 652 (1995).
 - ²¹ A. Schäfer, H. Horn, and R. Ahlrichs, *J. Chem. Phys.* **97**, 2571 (1992).
 - ²² K. Eichkorn, F. Weigend, O. Treutler, and R. Ahlrichs, *Theor. Chem. Acc.* **97**, 119 (1997).
 - ²³ A. D. Becke, *Phys. Rev. A* **38**, 3098 (1988).
 - ²⁴ J. P. Perdew, *Phys. Rev. B* **33**, 8822 (1986).
 - ²⁵ S. H. Vosko, L. Wilk, and M. Nusair, *Can. J. Phys.* **58**, 1200 (1980).
 - ²⁶ Y. Q. Xue, S. Datta, and M. A. Ratner, *Chem. Phys.* **281**, 151 (2002).
 - ²⁷ J. K. Viljas, J. C. Cuevas, F. Pauly, and M. Häfner, *Phys. Rev. B* **72**, 245415 (2005).
 - ²⁸ S. Datta, *Electronic Transport in Mesoscopic Systems* (Cambridge University Press, Cambridge, 1995).
 - ²⁹ F. Guinea, C. Tejedor, F. Flores, and E. Louis, *Phys. Rev. B* **28**, 4397 (1983).
 - ³⁰ A. W. Gosh, T. Rakshit, and S. Datta, *Nano Lett.* **4**, 565 (2004).
 - ³¹ A. Troisi and M. A. Ratner, *Nano Lett.* **4**, 591 (2004).
 - ³² L. F. Pacios and L. Gómez, *Chem. Phys. Lett.* **432**, 414 (2006).
 - ³³ F. Pauly, J.K. Viljas, J.C. Cuevas, and Gerd Schön, to be published (2007).
 - ³⁴ M. Kondo, T. Tada, and K. Yoshizawa, *J. Phys. Chem. A* **108**, 9143 (2004).
 - ³⁵ The fixing of all degrees of freedom in the contact structures (Fig. 2) except for the tilt angle φ will result in an overestimation of rotational energetic barriers.³⁷ This is clear, as the side groups cannot avoid each other for example by elongated lengths of the phenyl-ring-connecting carbon-carbon bonds. However, it needs to be kept in mind that in a metal-molecule-metal contact the presence of the metallic contacts puts additional constraints on the bridging molecule, possibly hindering such changes of the molecule's length. For the molecule R2 in isolation, experimental data yields rotational energy barriers $\Delta E_{0^\circ} = 40\text{--}84$ meV for $\varphi = 0^\circ$ and $\Delta E_{90^\circ} = 46\text{--}89$ meV for $\varphi = 90^\circ$ with respect to the ground-state energy (Refs. 36,37). In our gold-molecule-gold contacts we obtain barriers of $\Delta E_{0^\circ} = 70$ meV and $\Delta E_{90^\circ} = 134$ meV with respect to the energy minimum at the angle $\varphi_0 = 34^\circ$ (Fig. 4).
 - ³⁶ A. Almennigen, O. Bastiansen, L. Fernholt, B. N. Cyvin, S. J. Cyvin, and S. Samdal, *J. Mol. Struct.* **128**, 59 (1985).
 - ³⁷ S. Arulmozhiraja and T. Fujii, *J. Chem. Phys.* **115**, 10589 (2001).
 - ³⁸ The smaller tilt-angle intervals for S2 and D2 as compared with R2 are chosen to prevent the methyl groups from coming too close to each other. For S2 we rotate the molecule such that each methyl group passes a hydrogen atom, but we avoid the tilt angles where the two methyl groups would meet. Accordingly, for D2 φ is restricted even further.
 - ³⁹ J. C. Sancho-García and J. Cornil, *J. Chem. Phys.* **121**, 3096 (2004).
 - ⁴⁰ Due to our numerical grid with a finite resolution the averages in Eqs. (4) and (5) are indeed discrete sums over angles $\varphi_i = i \times \Delta\varphi$ with $\Delta\varphi = 2^\circ$.
 - ⁴¹ We take the thermal average $\bar{G}(T) = \langle G_\varphi(T) \rangle_\varphi$ (and $\langle G_\varphi(T = 0\text{ K}) \rangle_\varphi$) only over symmetry-nonredundant angle intervals, in which the ground-state tilt angle φ_0 of the gold-molecule-gold contacts of Fig. 2 is contained. Explicitly this means that for the molecules R2, S2, and D2 we consider the tilt-angle intervals $[0^\circ, 90^\circ]$, $[180^\circ, 300^\circ]$, and $[60^\circ, 120^\circ]$ of Fig. 4, respectively. In this way we can get rid of the unphysical symmetry violation of E_φ , visible in that figure. As explained in the text, this symmetry violation stems the fact that we have not performed a relaxation step for geometries deviating from the ground-state geometry with $\varphi = \varphi_0$ (Fig. 2). It should be clear that the energy landscape E_φ changes upon inclusion of such a relaxation step.³⁵
 - ⁴² For R2 the terms up to $m = 2$ need to be included in the Sommerfeld expansion of $G_\varphi(T)$ [Eq. (A1)], in order to describe the behavior of $\bar{G}(T) = \langle G_\varphi(T) \rangle_\varphi$ in Fig. 5. In contrast, for S2 and D2 already the $m = 1$ term is almost negligible as indicated by the close agreement of $\langle G_\varphi(T = 0\text{ K}) \rangle_\varphi$ and $\bar{G}(T)$.
 - ⁴³ G. K. Ramachandran, T. J. Hopson, A. M. Rawlett, L. A. Nagahara, A. Primak, and S. M. Lindsay, *Science* **300**, 1413 (2003).
 - ⁴⁴ N. W. Ashcroft and N. D. Mermin, *Solid state physics*, (Harcourt College Publishing, Orlando, 1976).
 - ⁴⁵ D. M. Bishop, *Group Theory and Chemistry*, (Dover, New York, 1993).
 - ⁴⁶ M. Wolfsberg and L. Helmholz, *J. Chem. Phys.* **20**, 837 (1952).
 - ⁴⁷ R. Hoffmann, *J. Chem. Phys.* **39**, 1397 (1963).
 - ⁴⁸ B. Tinland, *J. Mol. Struct.* **3**, 165 (1969).